

Transparent and flexible multi-layer films with graphene recording layers for optical data storage

Fei Xing, Xu-Dong Chen, Zhi-Bo Liu, Qian Zhang, Xiao-Qing Yan et al.

Citation: *Appl. Phys. Lett.* **102**, 253501 (2013); doi: 10.1063/1.4812473

View online: <http://dx.doi.org/10.1063/1.4812473>

View Table of Contents: <http://apl.aip.org/resource/1/APPLAB/v102/i25>

Published by the [AIP Publishing LLC](#).

Additional information on *Appl. Phys. Lett.*

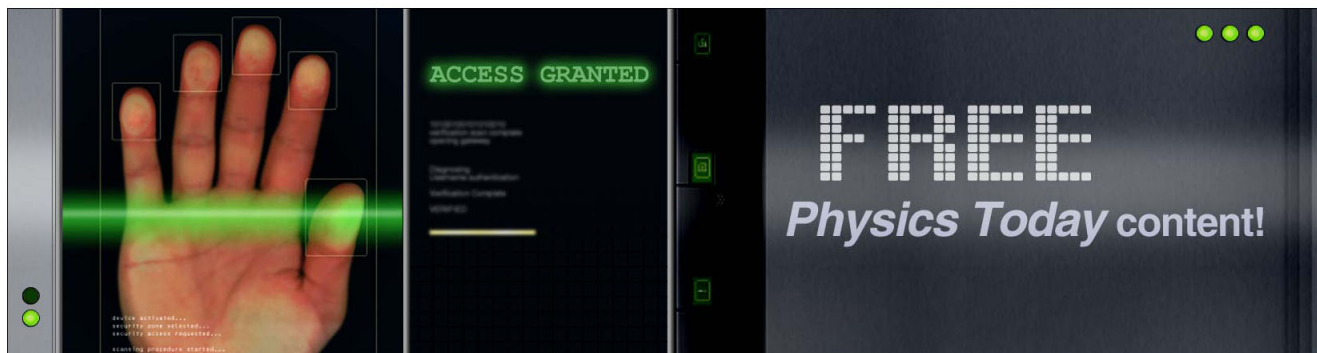
Journal Homepage: <http://apl.aip.org/>

Journal Information: http://apl.aip.org/about/about_the_journal

Top downloads: http://apl.aip.org/features/most_downloaded

Information for Authors: <http://apl.aip.org/authors>

ADVERTISEMENT



Transparent and flexible multi-layer films with graphene recording layers for optical data storage

Fei Xing,¹ Xu-Dong Chen,¹ Zhi-Bo Liu,^{1,a)} Qian Zhang,² Xiao-Qing Yan,^{1,2} Yongsheng Chen,² and Jian-Guo Tian^{1,b)}

¹The Key Laboratory of Weak-Light Nonlinear Photonics, Ministry of Education, School of Physics and TEDA Applied Physics School, Nankai University, Tianjin 300071, China

²The Key Laboratory of Functional Polymer Materials and Center for Nanoscale Science and Technology, Institute of Polymer Chemistry, College of Chemistry, Nankai University, Tianjin 300071, China

(Received 26 February 2013; accepted 9 June 2013; published online 24 June 2013)

Based on the polarization-sensitive absorption of graphene under conditions of total internal reflection, we demonstrate the fabrication and reading of transparent and flexible multi-layer-film optical data storage media based on graphene recording layers. We report a realization of the process of data writing-transferring-reading by repeatedly transferring recorded graphene and its strong polarization effect. The reading results show a high signal-to-noise ratio and stability and low crosstalk interference between the layers. In addition, the graphene-based multi-layer-film optical data storage medium has a high transparency and flexibility. The high signal-to-noise ratio remains stable after the structure is bent 1000 times. © 2013 AIP Publishing LLC.

[<http://dx.doi.org/10.1063/1.4812473>]

Optical data storage (ODS) represents revolutionary progress for the field of information storage capacity. Given the recent significant increase in the amounts of digital information being generated, the storage capacity of ODS media must improve further.¹ Therefore, the development of a high-density data storage medium has been increasingly pursued for ODS. At present, high-density ODS technology can be advanced in two ways: one way is to overcome the diffraction limit in order to improve areal storage density (e.g., near-field optical data storage).² The other approach for development is to establish a multi-layer data recording layer (DRL) in a three-dimensional (3D) optical data storage space to improve the volume storage density (e.g., two-photon 3D optical data storage and co-extruder multi-layer optical data storage).^{3,4} The number of DRLs in a finite thickness must be maximized to improve the volume storage so that more digital information can be stored with the same single-layer storage density. A challenge encountered in multi-layer ODS technology is crosstalk interference between layers. The requirements of multi-layer ODS in a developing process can be met by obtaining reading results with a high signal-to-noise ratio (SNR) and low crosstalk.

Graphene, a novel two-dimensional (2D) material, is a type of monolayer laminated structure composed of carbon atoms and is currently the thinnest known material.⁵ Graphene has been applied in optics, machinery, chemistry, and electronics.^{6–9} The thickness of monolayer graphene is 3.4 Å, and the optical transmittance of graphene is up to 97.7%.¹⁰ The carbon-atom plane can be bent and deformed to a large degree while maintaining a stable structure. Therefore, graphene is an ideal choice as a transparent and flexible active layer for ODS media. Currently, the microstructure size of graphene can be made to be a few tens of

nanometers or even several nanometers with the use of existing methods,¹¹ which allows for an areal storage density of up to 10¹² byte/cm². Furthermore, there are various methods for transferring graphene to an arbitrary flexible substrate.^{12–14} Consequently, graphene-based multi-layer-film ODS media can be achieved by repeatedly transferring graphene, and the volume storage density can be theoretically improved to 10¹⁵ byte/cm³–10¹⁷ byte/cm³. With regard to the writing and transfer of data in a graphene DRL, however, it is more difficult for graphene to be read out, especially for data that have been recorded on multi-layer films using the present optical methods because graphene is nearly transparent.

Under total internal reflection (TIR), the absorption of graphene for *s*-polarized light is much larger than that for *p*-polarized light.¹⁵ Based on this knowledge, a data reading device for multi-layer films was designed to read out data stored by a graphene-based multi-layer-film ODS medium. In this study, the data writing was performed on the graphene active layer based on photolithography and femtosecond (FS) laser direct writing technology. In the graphene transfer process, polydimethylsiloxane (PDMS) and hard-polydimethylsiloxane (h-PDMS) were used as flexible buffer layers to make the transparent and flexible multi-layer-film ODS medium. A balanced detector in the experiment converts the optical signals into electric signals and simultaneously amplifies them. The reading results show a high SNR and stability and low crosstalk interference between the layers. In addition, the graphene-based multi-layer-film ODS medium has a high transparency and flexibility.

Under TIR, the interaction between the evanescent wave and the material on the prism surface can change some of the properties of the reflected light, for example, via the surface plasma resonance effect.¹⁶ When there is graphene on the prism surface, the reflected *s*-polarized light intensity is much weaker than that of the *p*-polarized light after the TIR.¹⁵ In fact, for monolayer graphene, the *p*-polarized light intensity

^{a)}Author to whom correspondence should be addressed. Electronic mail: rainingstar@nankai.edu.cn

^{b)}jjitian@nankai.edu.cn

shows little variation with the presence of graphene on the prism surface under TIR. However, the *s*-polarized light intensity is approximately 9% lower than before reflection. When the light changes from *p*- to *s*-polarized, the reflectivity gradually decreases. The reflectivity of the *s*-polarized light is minimized, and the reflectivity difference between the *s*- and *p*-polarized light is maximized. For three-layer graphene, the reflectivity difference even reaches $\sim 20\%$ (Fig. S1).²² As a result, the data recorded in the graphene are likely to be read out with a high SNR. The reflectivity difference between the *s*- and *p*-polarized light is maximized at the graphene layer, and the corresponding voltage signal is recorded as “1.” The reflectivity difference between the *s*- and *p*-polarized light is minimized for the layer without graphene, and the corresponding voltage signal is recorded as “0.”

Because TIR occurs between an optically dense medium and an optically thin medium, once the high-low gradient of the refractive index is built between the buffer layers, the data from the multi-layer films can be read. Figure 1(a) shows the data-reading schematic diagram of the graphene-based multi-layer-film ODS medium. Because the refractive indices follow the order $n_1 > n_2 > n_3$, when the incident angle is large, TIR can first occur at the interfaces of the n_1 and n_2 media. Owing to the absorption difference for graphene between the *s*- and *p*-polarized light under TIR, the data recorded on the graphene between the interfaces of n_1 and n_2 can be read out. Next, when the incident angle is reduced to the correct angle range, the incident light can be totally reflected at the interfaces of n_2 and n_3 through the interfaces of n_1 and n_2 . Thus, the data recorded in the graphene between the interfaces of n_2 and n_3 are read out. Similarly, the data for the other layers can be read out.

In our experiment, three-layer graphene grown on a Ni substrate by chemical vapor deposition (CVD) is regarded as the active layer material. There are many methods for defining the number of graphene layers, such as transmittance methods, Raman spectroscopy,¹⁷ and surface plasmon resonance (SPR).¹⁸ Here, the number of graphene layers was

defined by the transmittance (Fig. S2) and Raman spectroscopy (Fig. S3). The absorbance of monolayer graphene is 2.3% and the absorbance of graphene samples we used is about 7% in the visible region. Therefore, the number of graphene layers is determined to be three. As a demonstration model, lithography technology¹⁹ was used to write microgrid structures as the data points. FS laser direct writing technology is also a good candidate for recording data in the graphene because submicron and even nanoscale data points can be fabricated by an FS pulse laser.²⁰ Figure 1(b) shows the setup of the data-writing process using an FS laser. Figure 1(c) shows a patterned graphene micrograph fabricated by ultraviolet photolithography technology. The microstructure of the graphene pattern written by the photolithography technology has a regular edge with a uniform band width. The width of the graphene band is $20\ \mu\text{m}$, and the distance between adjacent graphene bands is $50\ \mu\text{m}$. Figure 1(d) shows SEM image of three-layer graphene pattern fabricated by a FS pulse laser at 400 nm. A SEM image of monolayer graphene pattern fabricated by a FS pulse laser is shown in Fig. S5. The minimum distance between adjacent graphene bands is approximately 700 nm.

Owing to their excellent optical, mechanical, and surface chemical properties, PDMS and h-PDMS have been widely applied in optical fluidic chips, flexible devices, micro-fluidic chips, and soft lithography in recent years.²¹ The refractive index of PDMS is 1.4017, and the refractive index of h-PDMS is 1.4198 at room temperature. Thus, PDMS and h-PDMS can act as buffer layers with an index gradient. A graphene-based transparent and flexible multi-layer-film ODS medium was fabricated through the transfer process of graphene, as shown in Fig. 2(a). First, the h-PDMS prepolymer was poured onto a quartz substrate and spun. After curing the h-PDMS prepolymer, the h-PDMS surface was attached to Ni-based graphene with recorded data to form a structure of Si/SiO₂/Ni/graphene (G)/h-PDMS/quartz. The multi-layer structure was then soaked in an aqueous iron (III) chloride (FeCl₃) solution (1M) to

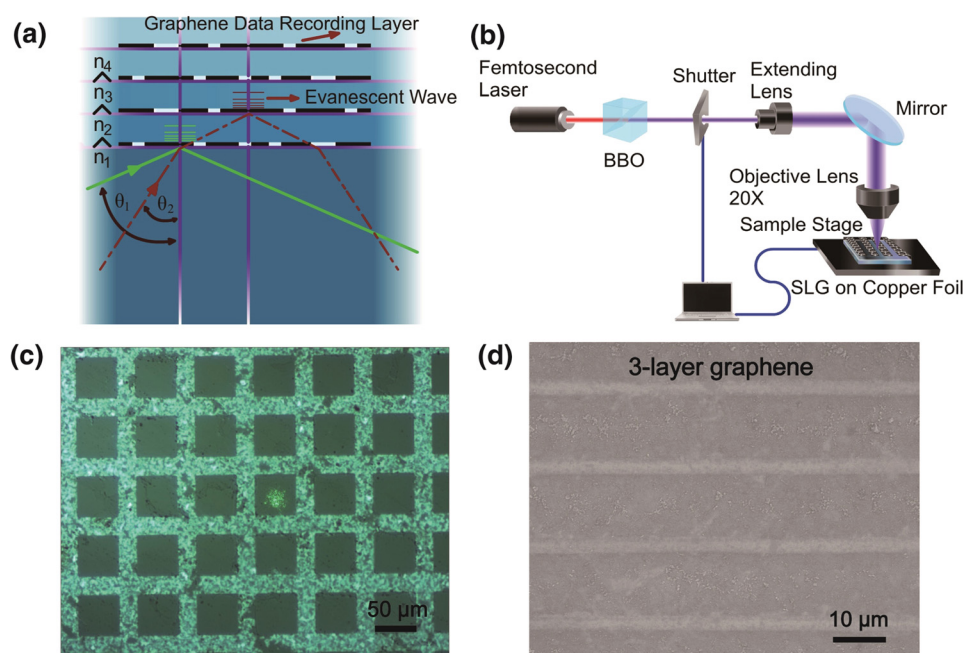


FIG. 1. (a) Data-reading schematic illustration of the graphene-based multi-layer-film ODS medium. (b) FS laser micromachining setup. (c) Patterned graphene fabricated by photolithography technology. The width of the graphene band is $20\ \mu\text{m}$, and the distance between adjacent graphene bands is $50\ \mu\text{m}$. The flexible substrate is PDMS with a light spot in the middle. (d) SEM image of the channel pattern for three-layer graphene on a PDMS flexible substrate.

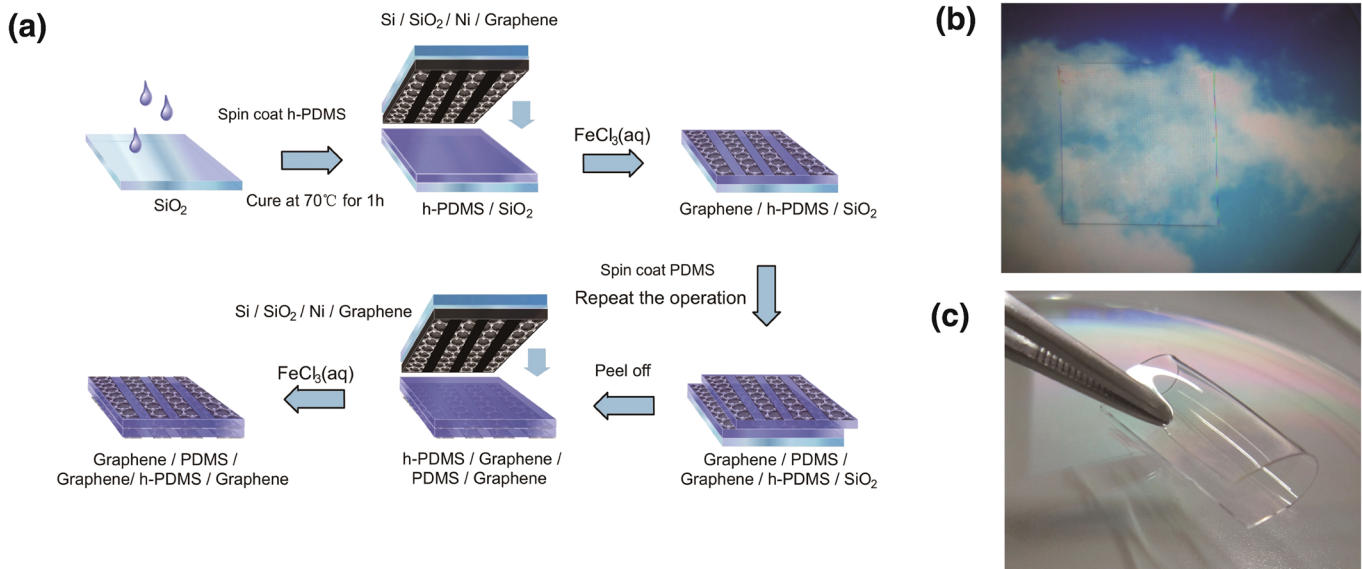


FIG. 2. Preparation of flexible three-layer-film ODS by repeatedly data transferring. (a) Schematic illustration of the experimental procedure for fabricating the transparent flexible graphene-based three-layer-film ODS medium. (b) and (c) Photographs of the transparent flexible graphene-based three-layer-film ODS medium.

remove the nickel layers. In this way, a 2D graphene-based ODS medium with h-PDMS as a buffer layer was obtained. By repeating the above process, three-layer ODS structures with h-PDMS and PDMS buffer layers can be obtained. Figure 2(b) displays a graphene-based three-layer-film ODS medium adhering to a liquid crystal display (LCD). The figure shows that this ODS structure has good transparency. Figure S6 shows the transmittance curves of the three-layer-film ODS medium and pure h-PDMS/PDMS buffer layers. The transmittances are higher than 75% at the visible band. Figure 2(c) shows that the three-layer ODS medium is sufficiently flexible.

Figure 3 shows a sketch diagram of the data-reading process for the multi-layer films. The graphene-based three-layer-film ODS medium was adsorbed on glass and formatted in the structure of glass ($n_1 = 1.5104$)/graphene/h-PDMS ($n_2 = 1.4188$)/graphene/PDMS ($n_3 = 1.4017$)/graphene/air ($n_4 = 1.0000$). The medium was placed on a prism ($n = 1.5104$) with an index-matching fluid between them. A continuous wave (CW) laser at 532 nm is transformed into circularly polarized light through a Glan-Taylor prism and a quarter-wave plate. Through objective focusing, the circularly polarized light is used to read the recorded data. The *s*- and *p*-polarized light components are separated by a polarized beam splitter. Therefore, the absorptions of graphene for the *s*- and *p*-polarized light are distinguished. The

variations in the *s*- and *p*-polarized light components are then simultaneously detected by a balanced detector, and the difference between the *s*- and *p*-polarized light intensities is converted into a voltage signal through the detector. The data recorded on each layer of graphene can be read out in a sequence by reducing the incident angle. Figure 4(a) displays the reading results of the graphene storage layer at the glass ($n_1 = 1.5104$) and h-PDMS ($n_2 = 1.4188$) interfaces. The zone corresponding to the low-voltage value without graphene is recorded as “0,” whereas the zone corresponding to the high-voltage value with graphene is recorded as “1.” The reading curves show that the voltage difference is more than 2 V between reading the “0” and “1” data, which indicates an ideal readout effect and a high degree of recognizable signal. The figure shows that the curves are smooth and that the heights of the regions in the “1” zone are nearly identical, which indicates that the signal is very stable during the readout process and that the transfer process has little impact on the graphene recording layer. The SNR for this reading method is approximately 100 based on the enlarged noise/signal figure.

Crosstalk interference between layers is a significant bottleneck for multi-layer-film ODS. In our experiments, the crosstalk interference between layers is mainly caused by two aspects. As shown in Fig. 1, the data stored by the graphene at the interfaces of n_2 and n_3 are taken as an example. One

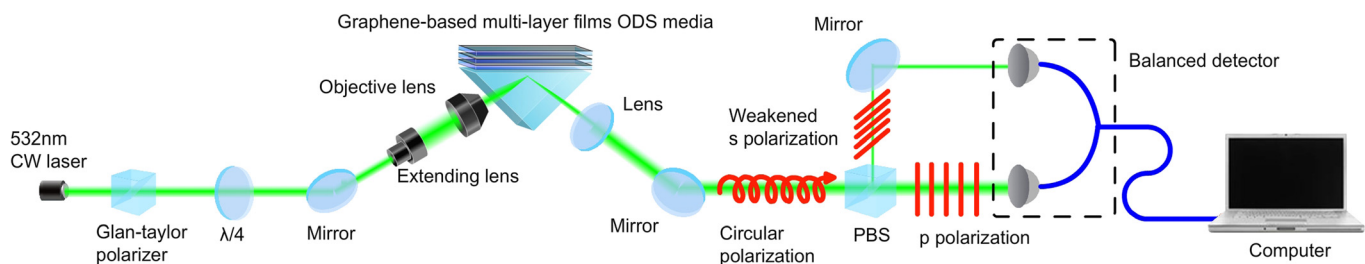


FIG. 3. A 532-nm CW laser is used for data reading. A polarized beam splitter (extinction ratio > 1000:1) divides the reflected light into *s*- and *p*-polarized light.

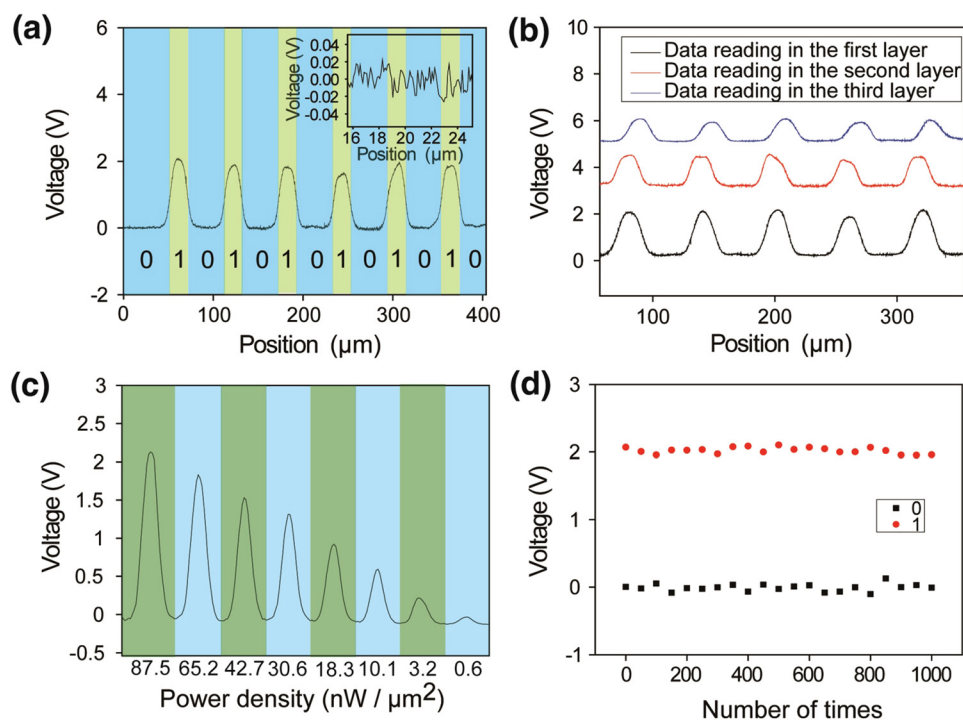


FIG. 4. (a) The modulation signal of the graphene storage layer at the glass ($n_1 = 1.5104$) and h-PDMS ($n_2 = 1.4188$) interfaces. The enlarged figure shows that the noise signal is 20 mV. (b) The reading results for each layer of the three-layer-film ODS medium. The buffer layer thickness of the h-PDMS and PDMS is $\sim 50 \mu\text{m}$. (c) The readout signal from the graphene recording layer between the glass ($n_1 = 1.5104$) and h-PDMS ($n_2 = 1.4188$) interfaces. The power density of the incident light ranged from $87.5 \text{ nW}/\mu\text{m}^2$ to $0.6 \text{ nW}/\mu\text{m}^2$. (d) Bending experiment of the graphene-based three-layer-film ODS medium at a power density of $87.5 \text{ nW}/\mu\text{m}^2$.

aspect is that part of the incident light is reflected and absorbed when it passes through the interfaces of n_1 and n_2 . Compared with the TIR, the absorption of the graphene is polarization-independent when the incident light passes through the graphene. The light intensity through the interfaces of n_1 and n_2 is weakened for both the s - and p -polarized light. Another aspect is due to the interaction between the evanescent wave and the graphene in the next layer when the evanescent wave passes through the interfaces of n_3 and n_4 . This result occurs because the evanescent wave decays exponentially in the direction perpendicular to the interface, and the general penetration depth is on the order of the incident light wavelength. Theoretically, if the thickness of the buffer layer is more than the wavelength of the incident light, the readout results cannot be influenced. Figure 4(b) shows the reading results of each layer of the three-layer-film ODS medium with a graphene recording layer. The buffer layer thickness of h-PDMS and PDMS is $\sim 50 \mu\text{m}$, which is orders of magnitude greater than the wavelength. The power density of the incident light is $87.5 \text{ nW}/\mu\text{m}^2$. The crosstalk interference between layers is very low because of the high SNR and the thick buffer layers. However, owing to the absorption and scattering of the graphene, the SNR decreases with an increase in the reading layers under the same reading intensity. The SNR is approximately 100 for the data on the graphene recording layer at the glass ($n_1 = 1.5104$) and h-PDMS ($n_2 = 1.4188$) interfaces, whereas the SNR reduces to 60 when the data on the graphene recording layer at the PDMS ($n_3 = 1.4017$) and air ($n_4 = 1.0000$) interfaces are read.

Figure 4(c) shows the readout signal from the graphene recording layer between the interfaces of glass ($n_1 = 1.5104$) and h-PDMS ($n_2 = 1.4188$) for a different incident light power. The figure shows that the larger the power density of the incident light, the higher the SNR of the reading results. When the power density of the incident light is $0.6 \text{ nW}/\mu\text{m}^2$, the SNR is approximately 5–6. This value corresponds to the

light power density of the minimum distinguished signal in the experiment.

A flexibility test was performed by repeatedly bending and relaxing this ODS medium around a solid column (radius = 10 mm), with a tensile strain of approximately 3%. Figure 4(d) shows that as the three-layer-film ODS medium is bent 1000 times, there is no significant electrical degradation in the “0” and “1” states. In this figure, the power density of the incident light was $87.5 \text{ nW}/\mu\text{m}^2$, and the interfaces of the prism ($n_1 = 1.5104$) and h-PDMS ($n_2 = 1.4188$) were tested. Note from the figure that the recording layer’s switch ratio is still stable after being bent 1000 times, and the voltage difference between the “0” and “1” states remains approximately 2 V.

In conclusion, we demonstrate the fabrication and reading of transparent and flexible multi-layer films ODS media based on graphene recording layers, an ultrathin two-dimensional carbon material. We report a realization of the process of data writing-transferring-reading by repeatedly transferring recorded graphene and strong polarization effect. The reading results show a high SNR and stability and low crosstalk interference between the layers. The voltage signal difference is more than 2 V between reading the “0” and “1” data. When the power density of the incident light is $0.6 \text{ nW}/\mu\text{m}^2$, the SNR is approximately 5–6. In addition, the graphene-based multi-layer-film ODS medium has a high transparency and flexibility. The high SNR remains stable after the structure is bent 1000 times. Since the data are point-by-point read out in the graphene data record layer, the data access rate is slower than that in the holographic data storage. However, a faster data access rate in such a graphene-based ODS is expected with the development of the data read methods, such as parallel read strategy.

The authors thank the Chinese National Key Basic Research Special Fund (Grant 2011CB922003), the Natural

Science Foundation of China (Grant 11174159), and the Natural Science Foundation of Tianjin (Grant 13JCYBJC16300).

- ¹H. Mustroph, M. Stollenwerk, and V. Bressau, *Angew. Chem., Int. Ed.* **45**, 2016 (2006).
- ²E. Betzig and J. K. Trautman, *Science* **257**, 189 (1992).
- ³J. Lott, C. Ryan, B. Valle, J. R. Johnson III, D. A. Schiraldi, J. Shan, K. D. Singer, and C. Weder, *Adv. Mater.* **23**, 2425 (2011).
- ⁴C. Ryan, C. W. Christenson, B. Valle, A. Saini, J. Lott, J. Johnson, D. Schiraldi, C. Weder, E. Baer, K. D. Singer, and J. Shan, *Adv. Mater.* **24**, 5222 (2012).
- ⁵K. S. Novoselov, A. K. Geim, S. V. Morozov, D. Jiang, M. I. Katsnelson, I. V. Grigorieva, S. V. Dubonos, and A. A. Firsov, *Nature* **438**, 197 (2005).
- ⁶A. Vakil and N. Engheta, *Science* **332**, 1291 (2011).
- ⁷M. I. Katsnelson, *Mater. Today* **10**, 20 (2007).
- ⁸A. K. Geim, *Science* **324**, 1530 (2009).
- ⁹S. Wang, P. K. Ang, Z. Wang, A. L. L. Tang, J. T. L. Thong, and K. P. Loh, *Nano Lett.* **10**, 92 (2010).
- ¹⁰R. R. Nair, P. Blake, A. N. Grigorenko, K. S. Novoselov, T. J. Booth, T. Stauber, N. M. R. Peres, and A. K. Geim, *Science* **320**, 1308 (2008).
- ¹¹X. Wang and H. Dai, *Nat. Chem.* **2**, 661(2010).
- ¹²J. W. Suk, K. Kirk, Y. Hao, N. A. Hall, and R. S. Ruoff, *Adv. Mater.* **24**, 6342 (2012).
- ¹³Y. Bie, Y. Zhou, Z. Liao, K. Yan, S. Liu, Q. Zhao, S. Kumar, H. Wu, G. S. Duesberg, G. L. W. Cross, J. Xu, H. Peng, Z. Liu, and D. Yu, *Adv. Mater.* **23**, 3938 (2011).
- ¹⁴J. B. Park, J.-H. Yoo, and C. P. Grigoropoulos, *Appl. Phys. Lett.* **101**, 043110 (2012).
- ¹⁵F. Xing, Z. Liu, Z. Deng, X. Kong, X. Yan, X. Chen, Q. Ye, C. Zhang, Y. Chen, and J. Tian, *Sci. Rep.* **2**, 908 (2012).
- ¹⁶P. Pattnaik, *Appl. Biochem. Biotechnol.* **126**, 79 (2005).
- ¹⁷D. Graf, F. Molitor, K. Ensslin, C. Stampfer, A. Jungen, C. Hierold, and L. Wirtz, *Nano Lett.* **7**, 238 (2007).
- ¹⁸S. Cheon, K. D. Kihm, J. S. Park, J. S. Lee, and B. J. Lee, *Opt. Lett.* **37**, 3765 (2012).
- ¹⁹L. Tapasztó, G. Dobrik, P. Lambin, and L. P. Biró, *Nat. Nanotechnol.* **3**, 397 (2008).
- ²⁰P. P. Pronko, S. K. Dutta, J. Squier, J. V. Rudd, D. Du, and G. Mourou, *Opt. Commun.* **114**, 106 (1995).
- ²¹D. Qin, Y. Xia, and G. M. Whitesides, *Nat. Protoc.* **5**, 491 (2010).
- ²²See supplementary material at <http://dx.doi.org/10.1063/1.4812473> for details of experiment and figures S1 to S6.